

"PROJECT FINALE" - SCREEN AND SCREEN PRINTING PROCESS DEVELOPMENT FOR ULTRA-FINE-LINE CONTACTS BELOW 20 μ m FINGER WIDTH

F. Clement^{a*}, M. Linse^a, S. Tepner^a, N. Wengenmeyr^a, L. Ney^a, K. Krieg^a, A. Lorenz^a, M. Pospischil^a, S. Bechmann^b, K. Oehrle^c, S. Steckemetz^d and R. Preu^a

- a) Fraunhofer Institute for Solar Energy Systems ISE, Heidenhofstraße 2, 79110 Freiburg, Germany
- b) Koenen GmbH, Otto-Hahn-Straße 24, 85521 Ottobrunn-Riemerling, Germany
- c) Kissel + Wolf GmbH, In den Ziegelwiesen 6, 69168 Wiesloch, Germany
- d) former: SolarWorld Industries GmbH, Carl-Schiffner-Straße 17, 09599 Freiberg, Germany

*Corresponding author: Florian Clement | Phone: +49 (0)761 4588 5050 | e-mail: florian.clement@ise.fraunhofer.de

ABSTRACT Within this work, a new model of the screen printing process is set up in order to improve the understanding of the screen printing process with focus on the interaction between -paste and -screen. First results show that wall slip behavior of the paste can be significantly improved by adapting the screen chemistry, enabling a lower finger resistances and reduced finger widths. A mean contact finger width of $w_{f\varnothing} = 26 \mu\text{m}$ combined with a mean finger resistance of $R_{\text{Finger}\varnothing} = 99 \Omega/\text{m}$ shows the high potential of the newly developed screen chemistry using single-step screen printing. Screen openings of $w_{\text{ch}} = 16 \mu\text{m}$ and printed finger widths of $w_f = 17 \mu\text{m}$ can be realized on textured Si wafers with ARC. Moreover, finger resistance values far below $R_{\text{Finger}} = 1000 \Omega/\text{m}$ are reached for nominal finger widths down to $w_f = 18 \mu\text{m}$. This proves the high potential of the single step screen printing process on the way to ultra-fine line contacts in combination with multi-busbar cell layouts. PERC-type Cz-Si solar cells fabricated with a 5 busbar cell layout and a nominal screen opening of $w_n = 24 \mu\text{m}$ achieve efficiencies up to $\eta_{\text{max}} = 22.1\%$. First multi-busbar solar cells with a $18 \mu\text{m}$ nominal screen opening demonstrate a significant Ag reduction.

Keywords: Metallization, Printing, Production Technology, Si solar cell

1 MOTIVATION

One of the main challenges within Silicon (Si) solar cell metallization is the decrease of finger width and silver (Ag) consumption. The research project FINALE starts right here. It is planned to significantly improve the front side metallization process as a key technology for the production of silicon solar cells. To this end, the screen printing technology established on the market is to be addressed. The technological limits of the printing process and the associated components are to be shifted in the direction of narrower contact widths ($<20 \mu\text{m}$) with sufficient contact height. The adaptation and optimization of the screen manufacturing process, but also of the screen chemistry, plays a central role in this. In addition to experimental work on printing parameter optimization, the development of a model for the theoretical description of the printing process is addressed in order to identify and optimize key influence factors in the printing process. Furthermore, the silver consumption in the screen printing process is improved by realizing contact fingers with an improved shape and homogeneity. The overall objective is a deep and interdisciplinary understanding of the printing process as a basis for further optimization. The reduction of process costs in $\text{€}/\text{Wp}$ is another central goal of the project, which is continuously monitored.

2 EXPERIMENTAL APPROACH

In this work, latest improvements concerning the flatbed screen printing process aiming at ultra-fine line contacts are presented.

A theoretic model is setup to understand the interactions between screen, paste, substrate and printing process itself. For this reason, a series on rheological investigations and printing experiments are performed to study the paste-screen interaction during the different phases within the screen printing process [1].

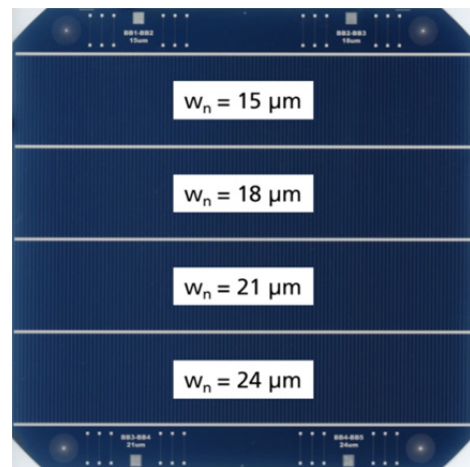


Figure 1: New designed test layout with 4 segments with decreasing nominal finger widths w_n (here: 15,18,21,24 μm) on one wafer. Distance and number of contact fingers corresponds to a typical solar cell layout and thus allows a direct inline measurement in an industrial I-V-tester.

The screen manufacturing process is improved in order to realize reproducible contact finger screen openings below $20 \mu\text{m}$ width. Various types of screen mesh and different screen chemistry (e.g. emulsions, surface coatings) are investigated in order to improve the screen properties for a reliable fine line printing process. Therefore, a test layout with 4 segments (decreasing nominal finger width w_n) is designed which allows an inline measurement of grid resistance (and thus mean finger resistance) for each nominal finger width (fig. 1).

Finally, PERC (passivated emitter and rear contact) type Si solar cells are produced and characterized in order to demonstrate high solar cell efficiencies and a lower Ag consumption.

3 RESULTS & DISCUSSION

3.1 Theoretic investigation of the screen printing process

A theoretical multi-dimensional model of the screen printing process is set up in order to understand the screen printing process in more detail. The model will be developed in three steps:

- 1) Fluid-Structure interaction:
The paste-screen interaction is investigated to derive design goals for wire and emulsion surface properties which will optimize the flow and slip behavior of metal pastes during the different process phases in screen printing.
- 2) Modeling of the screen architecture:
A model is developed which predicts the size, the geometric form and the exact location of all individual openings within a screen channel and their dependency on all screen design parameters (e.g. Mesh count, wire diameter, screen angle, screen opening width)
- 3) Combination of 1) and 2) in order to model and optimize the entire screen printing process on the Si-wafers.

Up to now, the focus lies on the first and second step. Tepner et al. showed that the interface between the paste and emulsion surface requires significant slip behavior when an optimized screen snap-off during printing is desired [1]. In that study, a functional coating is applied onto the screen (emulsion surface and mesh wires) by plasma-enhanced physical vapour deposition (PECVD). The surface properties of the applied coating allow for an increased paste transfer and reduced spreading on the substrate. In order to verify this hypothesis, contact angle measurements of respective paste solvents were carried out and the corresponding work of adhesion W_a on the surface was calculated. Table 1 presents the measurements of contact angles θ of the paste solvent A on various coated surfaces. An exponential correlation between the work of adhesion W_a and the ability to slip at the coated emulsion surface was discovered. At high contact angles, the work of adhesion between the surface and paste solvent is reduced, resulting in an increased slip velocity at the paste-emulsion interface. Therefore, more paste volume is pushed into the screen channel during the flooding phase of the screen printing process. Furthermore, high slip velocities during the snap-off mechanic will result in a reduction of induced shearing forces into the paste sample. By achieving this flow behavior, the critical yield stress of the paste will not be surpassed and therefore, potential spreading on the substrate will be reduced or prevented.

For this reason, the two best paste-coating candidates were tested during screen printing. In Figure 2, metallization results of Paste A with three different screens (uncoated reference, coating C and coating D) are presented, revealing a significant reduction of the printed finger width w_f due to less spreading on the substrate. Furthermore, for the $27\mu\text{m}$ wide screen opening the paste transfer is increased, resulting in an increased cross sectional area A_f of the printed contact finger and a reduced lateral finger resistance R_{Finger} respectively.

Table 1: Measurement results of the contact angle for the paste solvent of paste A on different surfaces.

Paste	Steel (°)	Coat. A (°)	Coat. B (°)	Coat. C (°)	Coat. D (°)
Solvent	14.3	16.7	36.1	52.9	58.3
Paste A	± 1.3	± 2.7	± 0.9	± 1.8	± 2.0

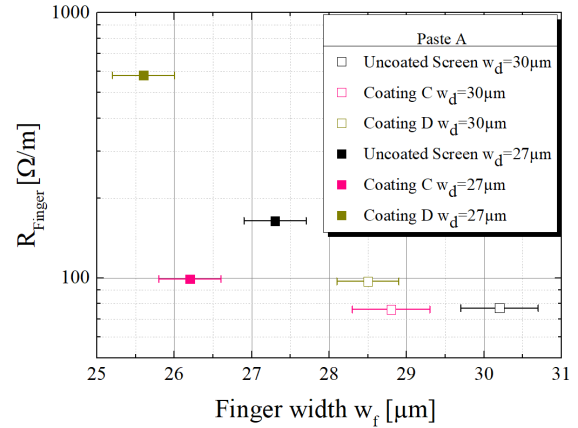


Figure 2: The correlation between the printed finger width w_f and the corresponding lateral finger resistance R_{Finger} is presented. The application of coating C results in a significant reduction of the printed finger width w_f due to less spreading on the substrate. Furthermore, for the $27\mu\text{m}$ wide screen opening the paste transfer is increased because of an optimized slip behavior at the paste-emulsion interface. For coating D with a screen opening of $27\mu\text{m}$, some challenges during the manufacturing process need to be resolved in order to ensure a sufficient printing result.

For the second step of the presented theoretical model of the screen printing process, Ney et al. developed a screen simulation approach, which is able to investigate the dependency of the open area OA_1 within a screen opening on all relevant screen design parameters (e.g. channel length, mesh count, wire diameter, screen opening width, position on the screen) [2]. Figure 3 (top), illustrates the definition of the parameter σ_{OA} , which describes how much the open area deviates from the mean value across the channel length. On the bottom of Fig. 3, simulation results for different screen angles and screen opening widths are presented, revealing that high screen angles will promise less deviation of the open area OA_1 at small screen openings. This result indicates that a further reduction of the lateral finger resistance R_{Finger} is expected because local reductions of the printed finger height will be minimized. Furthermore, Tepner et al. expanded on this simulation approach to investigate the existence of wire crossings in screen openings. He showed that this simulation method can be used to find screen patterns with extraordinary features (e.g. knotless configurations at screen angles above 0° without the drawbacks of conventional knotless screens) [3]. In future studies the presented approaches and results will be combined in order to optimize the screen printing process in terms of the printing performance, the throughput rate and the cost and the reliability of the screen manufacturing process.

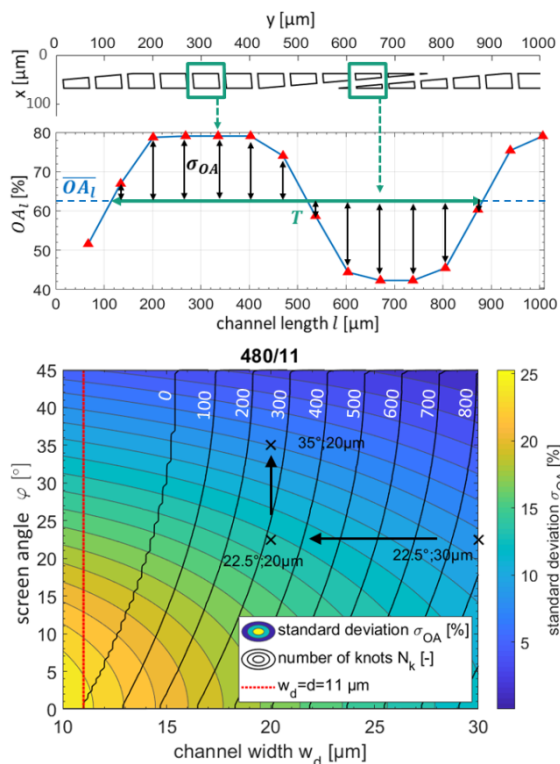


Figure 3: On the top, the simulated oscillating behavior of the local open area OA_l (blue curve) along the channel length l with screen angle $\varphi = 5^\circ$ and $w_d = 30 \mu\text{m}$ is shown. As a result, the standard deviation σ_{OA} of the local open area can be derived. On the bottom, the dependency of this deviation σ_{OA} and the number of knots (contour lines) on the screen angle φ and channel length w_d with constant mesh count of $MC = 480$ 1/inch and constant wire diameter of $d = 11 \mu\text{m}$ is presented.

3.2 Screen evaluation

Several screens with different screen parameters (mesh count, wire diameter, screen chemistry, screen angle, etc.) are evaluated.

In the first run, the focus lies on the identification of screen parameters for a reliable front side metallization process with single-step screen printing using a 5 busbar layout. A screen configuration (380-0.014, coating C) with a nominal finger width of $w_n = 30 \mu\text{m}$ was identified as an optimal starting point and was used for solar cell processing (see next chapter).

The second run aims at the realization of contact fingers with finger widths below $w_f = 20 \mu\text{m}$ and less finger interruptions suitable for a multi-busbar (>5) front side metallization. Selected test results are shown in the following figures (fig 4-6). Finger openings/widths below $20 \mu\text{m}$ are achieved in the screen and on textured Si wafers with ARC. Finger resistance values far below $R_{\text{Finger}} = 1000 \Omega/\text{m}$ using a 480-0.011 screen mesh show that nominal finger widths w_n down to $18 \mu\text{m}$ can be printed with sufficiently low for solar cells with a multi-busbar layout. The values for w_n of $21 \mu\text{m}$ and $24 \mu\text{m}$ allow the realization of 5 or 6 busbar cells. However, a nominal finger width of $w_n = 15 \mu\text{m}$ is still challenging for a reliable solar cell metallization using a single step screen printing process.

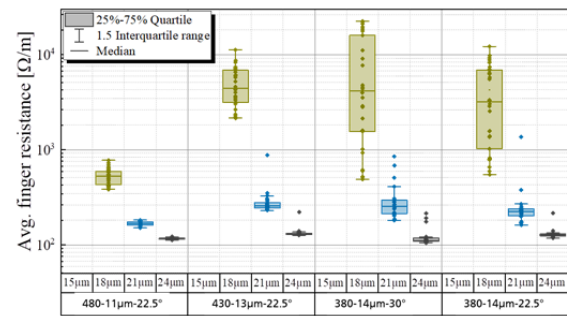


Figure 4: Finger resistance values for 4 different screens with 4 different nominal finger widths on each screen (see Fig 1). For a nominal finger width w_n of $15 \mu\text{m}$ no measurement is possible due to inhomogeneities of the printed finger lines. The lowest values are achieved using the 480-0.011 mesh (mesh wire diameter: $11 \mu\text{m}$)

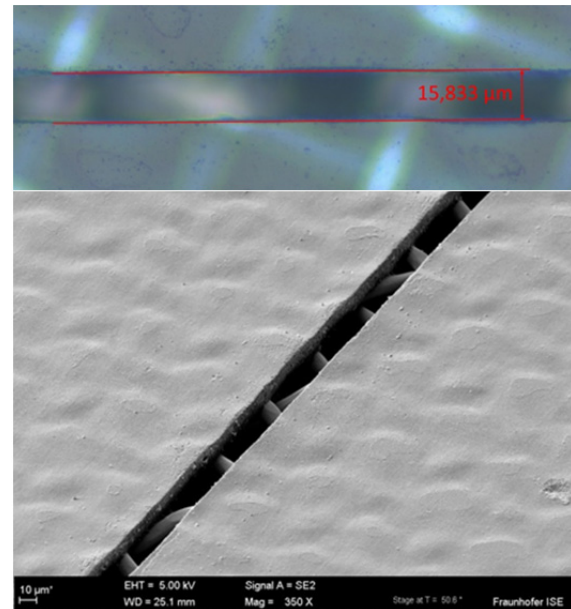


Figure 5: top: Selected 2D measurement of a screen with 480-0.011 mesh (mesh wire diameter $11 \mu\text{m}$) with screen chemistry coating C. The measured screen opening is $w_{ch} = 15.8 \mu\text{m}$ for a nominal finger width of $w_n = 15 \mu\text{m}$. bottom: selected SEM image of a screen with 480-0.011 mesh (mesh wire diameter $11 \mu\text{m}$) with screen chemistry coating C.

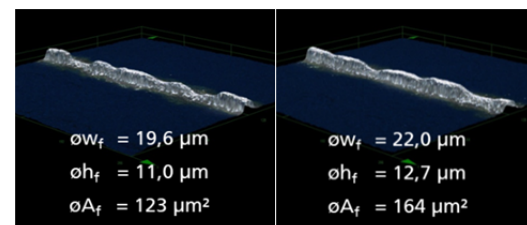


Figure 6: Selected 3D microscope measurement of a single step screen printed contact finger on a textured Si wafer with ARC, printed using a 480-0.011 mesh with screen chemistry coating C and nominal finger width of $w_n = 15 \mu\text{m}$ (left) and $w_n = 18 \mu\text{m}$ (right). The measured mean values for the finger width w_f , height h_f and cross section A_f are listed.

3.3 Solar cell results

Within this work, Cz-Si PERC type solar cells were fabricated at the pilot line of Solarworld and in the PV-TEC Back End lab at Fraunhofer ISE. Within the test runs carried out at Solarworld, only the nominal finger width in the screen has been varied (27 μ m, 30 μ m). Within the experiment at PV-TEC, 4 different screens have been used in three different print runs (360-0.016 mesh, 380-0.014 mesh, 440-0.013 mesh “knotless”, 480-0.011 mesh). Only in run “2018”, the same screen parameters and screen chemistry has been used in comparison to the runs at Solarworld. In run “2019” a 5 busbar and a busbarless cell layout has been realized. It must be noted, that different Cz-Si wafers and front-end processes have been used at Solarworld and PV-TEC. The PV-TEC process flow and cell results are presented in figure 7. The Solarworld cell results in table 2. The best cell efficiency of $\eta_{max} = 22.1\%$ (screen 430-0.013 mesh “knotless”) has been independently confirmed by Fraunhofer ISE CaLLab.

The PV-TEC results demonstrate a significant efficiency increase of almost $\Delta\eta = 1\%$ abs. and at the same time a clear reduction of the printed finger widths as well as of the Ag consumption in comparison to the starting point in run “2017”. An Ag reduction of around 35% for the 5 busbar layout from “2017” to “2019” and a printed finger width of $w_f = 22\mu$ m for the multibusbar cell layout in run “2019” underline the high potential of the newly developed fine line screens.

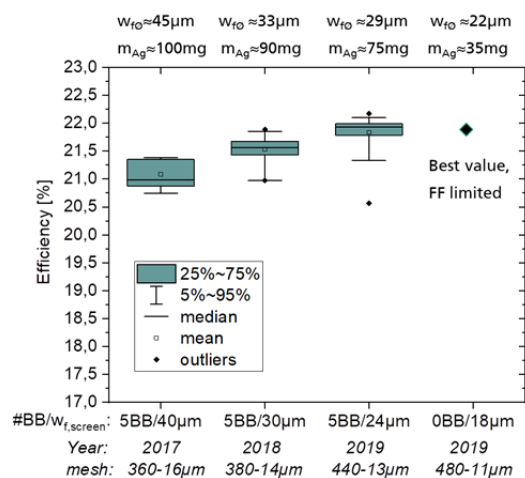
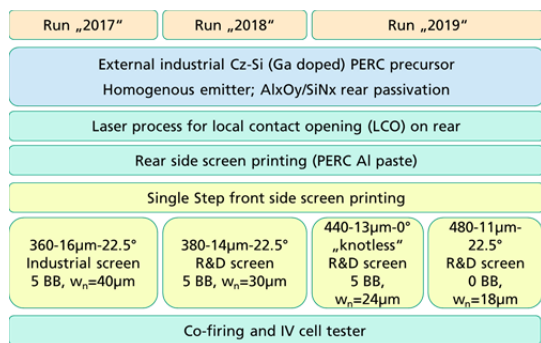


Figure 7: PV-TEC Back End lab: experimental process flow (top); cell efficiencies as well as mean values for the finger widths and Ag consumption (paste laydown, wet) for 4 different screens (bottom).

Table 2: IV Results of the test run at Solarworld pilot line: Around 50 cells per group; front end process with selective emitter:

w_n (μ m)	R_{Finger} (Ω /m)	$m_{Ag,wet}$ (mg)	J_{SC} (mA/cm ²)	FF (%)	V_{OC} (mV)	eff_{mean} (%)
30	86	103	40.0	80.8	676	21.9
27	120	92	40.1	80.6	677	21.9

4 SUMMARY AND OUTLOOK

Within this work a new theoretic model of the screen printing process is set up in order to improve the understanding of the screen printing process itself, especially of the interaction between the paste and the screen. First results show that wall slip behavior of the paste can be significantly improved by adapting the screen chemistry. This allows for a reduction of the average finger resistances at reduced finger widths. A mean contact finger width of $w_{f\varnothing} = 26 \mu$ m combined with a mean finger resistance of $R_{Finger\varnothing} = 99 \Omega$ /m shows the high potential of the newly developed screen chemistry using single-step screen printing. Screen openings of $w_{ch} = 16\mu$ m and printed finger widths of $w_f = 20\mu$ m can be realized on textured Si wafers with ARC. Moreover finger resistance values far below $R_{Finger} = 1000 \Omega$ /m are reached for nominal finger widths down to $w_n = 18\mu$ m. This proves the high potential of the single step screen printing process on the way to ultra-fine line contacts in combination with multi-busbar cell layouts. PERC type Cz-Si solar cells fabricated with a 5 busbar cell layout and a nominal screen opening of $w_n = 24\mu$ m achieve efficiencies up to $\eta_{max} = 22.1\%$. First multi-busbar solar cells with a 18 μ m nominal screen opening demonstrate a significant Ag reduction.

5 ACKNOWLEDGEMENT

The authors would like to thank all co-workers at the Photovoltaic Technology Evaluation Center (PV-TEC) at Fraunhofer ISE as well as at Koenen, Kissel+Wolf and Solarworld for supporting this work.

This work was partly financed by the by the federal ministry of economic affairs within the FINALE project funded under the contract number 0324098B.

6 REFERENCES

- [1] S. Tepner, N. Wengenmeyr, L. Ney, M. Linse, M. Pospischil, F. Clement, “Improving Wall Slip Behavior of Silver Pastes on Screen Emulsions for Fine Line Screen Printing”, Solar Energy Materials and Solar Cells (2019).
- [2] L. Ney, S. Tepner, M. Linse, A. Lorenz, S. Bechmann, R. Weber, M. Pospischil, F. Clement, Optimization of Fine Line Screen Printing Using in-depth Screen Mesh Analysis, AIP Conference Proceedings (2019)
- [3] S. Tepner, L. Ney, M. Linse, A. Lorenz, M. Pospischil, F. Clement, “Studying Alternative Knotless Screen Patterns for Fine Line Screen Printing of Si-Solar Cells” (2019) (to be published)